Automated IMT estimation and BMI correlation using a low-quality carotid ultrasound image database from India

Filippo Molinari, *Member IEEE*; Vipin Gupta; Poornima Prabhakaran; Kristen M. Meiburger, *IEEE Graduate Student Member*; Luca Saba; U. Rajendra Acharya, *Senior Member IEEE*; Giuseppe Ledda; K.V. Radha Krishna; Gagandeep Kaur Walia; Sanjay Kinra; Andrew Nicolaides; Shah Ebrahim; Jasjit S. Suri, *Senior Member IEEE*, *Fellow AIMBE*

***Abstract*— This paper presents AtheroEdgeLowRes (AELR), an extention of AtheroEdge™ from AtheroPoint™, and a solution to carotid ultrasound IMT measurement in low-resolution and overall low quality images. The images were collected using a low-end ultrasound machine during a screening study in India. We aim to demonstrate the accuracy and reproducibility of the AELR system by benchmarking it against an expert Reader's manual tracing and to show the correlation between the automatically measured intima media thickness (IMT) and the subjects' cardiovascular risk factors (i.e. body mass index – BMI). We introduced an innovative penalty function (PF) to our dual-snake segmentation technique, necessary due to the low image resolution. We processed 512 images from 256 patients, and correlated the AELR IMT values with the patients' age and BMI. AELR processed all 512 images, and the IMT measurement error was 0.011±0.099 mm with the PF correction and 0.173±0.127 mm without. AELR IMT values correlated with the Reader's values (r = 0.883) and also correlated with the subject's BMI and age. The AELR system showed accuracy and reproducibility levels that make it suitable to be used in large epidemiological and screening studies in emerging countries.**

I. Introduction

Atherosclerosis is a subtle and progressive degeneration of the artery walls leading to increase of the wall size, narrowing of the lumen, reduction of the blood flow and impairment of the artery compliance [1]. Though atherosclerosis was prominently a problem of the developed countries [2], its impact is increasing even in emerging and third world countries [2, 3]. Ultrasound imaging is the most widely used and established diagnostic and screening technique for atherosclerosis [4]. Ultrasound scanners are relatively cheap and portable [4], making it an affordable screening technique even in low-income countries. An expert operator usually manually measures the IMT by tracing the lumen-intima (LI) and media-adventitia (MA) interfaces. However, manual measurements are discouraged in multi-center and epidemiological studies because they are user-dependent, not fully standardized, time-consuming and prone to errors [4].

Recent studies showed that computer systems could be very useful in reducing the inter-reader variability associated to carotid IMT measurements [5]. Polak *et al.* proposed that computer algorithms for the measurement of the IMT had to be not only accurate, but also had to maintain the cardiovascular risk factor of the subjects and provide a reliable stratification of the patients' vascular age [5].

In a previous study, we showed that when low-end scanners are used, the acquired images often represent a difficult challenge to automated segmentation techniques, due to limited contrast and the fact that the LI/MA interfaces might be discontinuous and interrupted [2]. In this study we used a technique based on deformable parametric models (called *snakes*) [6], already presented and benchmarked in other studies [7]. The advantage of snakes is the possibility of imposing a regularization of the profile, which is very useful in presence of little visible or interrupted LI/MA interfaces. Snakes are, however, very sensible to image superimposed noise and need an accurate initialization [8].

The first objective of this work was the development of an accurate dual-snake model for the segmentation and IMT measurement of low-resolution carotid images. The second objective of this study was the evaluation of the automated snake system on a screening dataset and its correlation of the automatically measured IMT with the patients' risk factors, particularly with the subject's body mass index (BMI) which showed a clear association with atherosclerosis [9].

II. Materials and Methods

A. Patients Demographics and Image Acquisition

The image database consisted of 512 images, taken from 256 patients in India. The data acquisition was conducted in rural villages of India under the framework of the Andhra Pradesh Children and Parent Study (APCAPS) study. Table I summarizes the demographics of the patients. Of the 256 initial patients, 201 were examined a second time one year later and 55 were examined two years later.

F. Molinari and K. M. Meiburger are with BioLab, Dept. of Electronics and Telecommunications, Politecnico di Torino, 10129, Torino, Italy (corresponding author; phone: +39-(0)11-090-4135; fax: +39-(0)11-090-4217; e-mail: filippo.molinari@polito.it).

V. Gupta is with the the Public Health Foundation of India, New Delhi, South Asia Network for Chronic Disease.

P. Prabhakaran and S. Ebrahim are with the University of Bristol.

L. Saba and G. Ledda are with the Department of Radiology, Azienda Ospedaliero Universitaria (A.O.U.), Cagliari, Italy.

U. R. Acharya is with the Department of ECE, Ngee Ann Polytechnic, Singapore.

K.V. Radhakrishna is with the Division of National Institute of Nutrition, Indian Council of Medical Research.

G. K. Walia is with the South Asia Network for Chronic Disease, Public Health Foundation of India.

S. Kinra is with the Wellcome Trust, Public Health Foundation of India.

A. Nicolaides is with the Vascular Diagnostic Center, Nicosia, Cyprus.

J. S. Suri, is with Point of Care Division, Global Biomedical Technologies Inc., CA, USA, and Stroke Screening and Monitoring Division, AtheroPoint LLC, CA, USA and also affiliated with Idaho State University, Pocatello, ID, USA (e-mail: jsuri@comcast.net).

The carotid images were acquired by using a low-end ultrasound scanner (Ethiroli Tiny-16a, Surabhi Biomedical Instrumentation, Coimbatore, India) equipped with a linear transducer working in the frequency range 5-10 MHz. The subjects were scanned while in supine position.

All the images were in JPEG format and had a vertical pixel density equal to 12.7 pixels/mm, which is typical for a low-end OEM ultrasound scanner. Therefore, the pixel to mm conversion factor (CF) for the images was 0.0787 mm/pixel. Usually, the CF for medium-end OEM scanners is approximately 0.065 mm/pixel [10].

TABLE I - DEMOGRAPHICS OF THE PATIENTS

Number of patients	256
Sex	139 males, 117 females
Age	35.0 ± 14.6 years, range 10-65 years
Hypertension	12
Diabetes	6
Heart disease	5
Stroke	4
Asthma	2
BMI (kg/m^2)	20.3 ± 3.5, range 13.2-32.4

B. Manual Tracings

An expert radiologist (L.S.) manually traced the far wall LI and MA boundaries by using graphical user interface [7]. The manually traced LI/MA profiles by the expert Reader were considered as ground-truth. All the distance measurements between profiles were made by using the Polyline Distance Metric (PDM) [11].

C. LI/MA Segmentation using Dual-Snake Framework and Penalty Function

The segmentation strategy we used was based on an innovative dual-snake formulation we proposed in 2012 [7] and named CMUDS (Carotid Measurement Using Dual Snake). In the following we summarize the structure of AtheroEdgeLowRes (AELR) and highlight the technical innovation we brought to make AELR accurate on this database of low-resolution images.

1. AtheroEdgeLowRes architecture

AtheroEdgeLowRes (AELR) is completely automated and consists of the following three stages:

Stage 1: Far adventitia tracing. Initially, the far wall adventitia layer (AD_F) was automatically traced by means of a recognition system based on first-order Gaussian filtering and multi-resolution approach [12].

Stage 2: Dual snake initialization and LI/MA profiles tracing by dual-snake technique. Both the LI and the MA snakes were automatically initialized by using the AD_F profile traced in Stage 1. So, the two snakes initially had the same shape and number of points. We adopted a snake mathematical model as we described in [7]:

$$E(v(s)) = \int_0^1 \alpha|v'(s)|^2 + \beta e(v(s)) + \gamma|(v(s)) - e(v(s))|ds \quad (1)$$

where $v(s)$ represents the snake in a normalized coordinate space s in the range [0,1]. The first term of (1) is the internal energy. The second term is an external energy, in which the functional $e(x, y)$ is an edge operator called FOAM (First Order Absolute Moment). FOAM has already been used for the detection of LI/MA edges and, with respect to traditional gradients, is more accurate in representing the wall borders and less sensitive to image noise [12]. The last term of (1) is an attraction term used to drive the snake towards the actual position of the LI/MA interfaces. This term computes the distance between the edges $e(x, y)$ of the image and the snake position $v(s)$, so even if the snake is placed in a region where FOAM is null, it is attracted by its closest edge. So, there was a total of six parameters: α (curvature), β (stopping energy), and γ (attraction energy) for the LI snake (equal to 0.5, 0.1, 0.1, respectively) and α, β, and γ for the MA snake (equal to 0.5, 0.2, 0.05, respectively).

Stage 3: Dual-snake evolutions under mutual constraint. Since snakes could either collapse or diverge excessively, we constrained their mutual distance during evolution. When a point had a distance exceeding 3 mm (upper threshold) or lower than 0.3 mm (lower threshold), the point was shifted towards or away from, respectively, the MA snake until its distance was within the thresholds [7].

2. LI/MA Correction using Penalty Function (P)

Since this carotid ultrasound was low-resolution (pixel density of 12.7 pixels/mm), the AELR performance was sub-optimal for this set of images. We introduced a correction factor, which was correcting the penalty due to the overall poor image quality and resolution. We called it "Penalty Correction Factor or Penalty Function". In fact, one pixel had the vertical dimension of 0.0787 mm; therefore, if the IMT measurement error were equal to 1 pixel in an image, it would be of 0.0787 mm. This means that considering a normal value of IMT equal to 0.8 mm [13], 0.0787 mm would be approximately 10%. The P was defined as:

$$P = W \cdot R \quad (2)$$

where P is the average penalty factor and is computed by measuring the average PDM between the AELR LI/MA profiles and the manual LI/MA tracings by the Reader on a training data sets. In (2), R is the pixel resolution (0.0787 mm/pixel), whereas W is the weight factor to be applied to the computer generated LI/MA profiles. We made a pilot test on a set of 800 images acquired by the same scanner that

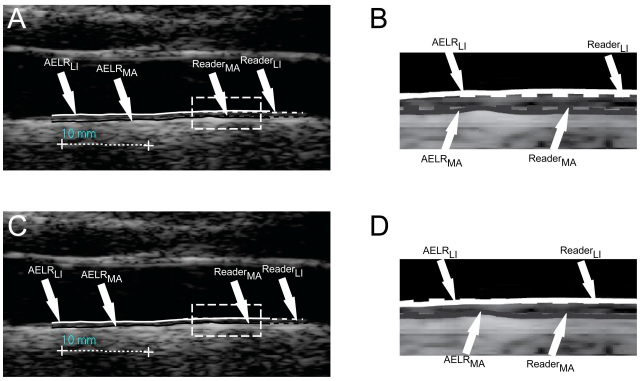

Fig. 1. Example of the PF correction applied to AtheroEdgeLowRes (AELR) LI/MA tracings. The white dashed rectangles show an image region that is represented zoomed in the side panels. LI profiles are in white, MA in black. A) AELR LI/MA profiles prior to PF correction vs. the manual Reader's tracings (dashed lines). B) Zoomed image region of Panel A. C) AELR LI/MA profiles after the PF correction compared to the manual Reader's tracings (dashed lines). D) Zoomed image regions of Panel C. AELR tracings are accurate and almost perfectly overlapped to the Reader's tracings.

was used to acquire the 500 images of this study, which were used in an epidemiological study [2], and we found that the *W* value that optimized the penalty factor was equal to 0.9. This resulted in a PF for the LI snake equal to 1.8491 ± 5.9957 pixels, and equal to 2.2742 ± 5.6069 pixels for the MA snake. These PFs (P) were then applied after CMUDS computed the LI/MA borders on the test 500 images.
Fig. 1 shows an example of the effect of the PF correction.

III. RESULTS

A. Performance Evaluation of AtheroEdgeLowRes: Comparison against Reader

AELR correctly processed all the 512 images of the dataset. Figure 2.A reports the correlation plot of the AELR IMT and of the Reader's measurements; the correlation coefficient is 0.8834 (95% C.I.: 0.854 – 0.907). Table II reports the IMT values measured by AELR and by the Reader subdivided for the different patient's pathologies. When we considered the entire set of 512 images, the average IMT value measured by AELR was 0.593 ± 0.140 mm, whereas that of the Reader was 0.604 ± 0.129 mm. The IMT measurement error was 0.011 ± 0.099 mm and was statistically not different from zero ($p > 0.8$). Table II shows that there is an overall good agreement between the two measurements and the average IMT values were never statistically significant (*p* always higher than 0.1).

TABLE II - IMT MEASUREMENT PERFORMANCE OF AELR COMPARED TO THE READER FOR THE ENTIRE DATASET AND IN FUNCTION OF SEX, HYPERTENSION, DIABETES, HEART DISEASE, STROKE, AND ASTHMA

	AELR IMT (mm)	**Reader IMT (mm)**
All 512 images	0.593 ± 0.140	0.604 ± 0.129
Sex		
Male (N = 139)	0.592 ± 0.123	0.607 ± 0.119
Female (N = 117)	0.569 ± 0.109	0.579 ± 0.089
Hypertension		
YES (N = 12)	0.615 ± 0.043	0.613 ± 0.061
NO (N = 244)	0.576 ± 0.111	0.587 ± 0.096
Diabetes		
YES (N = 6)	0.671 ± 0.174	0.709 ± 0.193
NO (N = 250)	0.580 ± 0.115	0.591 ± 0.103
Heart disease		
YES (N = 5)	0.654 ± 0.118	0.648 ± 0.081
NO (N = 251)	0.508 ± 0.117	0.593 ± 0.107
Stroke		
YES (N = 4)	0.789 ± 0.182	0.790 ± 0.261
NO (N = 252)	0.579 ± 0.113	0.590 ± 0.101
Asthma		
YES (N = 2)	0.612 ± 0.097	0.577 ± 0.009
NO (N = 254)	0.581 ± 0.117	0.594 ± 0.108

The accuracy of the IMT measurements by AELR can also be seen in the Bland-Altmann plot of Fig. 2.B, where no significant trend is present and an overall good agreement between AELR and the Reader can be observed. Example segmentation results can be seen in Fig. 3.

B. Carotid IMT Association with BMI and Age

We correlated the AELR and Readers IMT values to the BMI and age of the subjects, to evidence possible association between the computer measurements and the patient's demographics for these low-resolution images. Figure 4.A and 4.B reports the correlation plots for the AELR and Reader (IMT measurements and the subject's BMI. Figure 4.C and 4.D reports the correlation plots between the AELR and Readers IMT measurement with respect to the patients' age. It can be noticed that the correlation plots consist of two distinct clouds of points. This is due to the fact that the specific data were acquired during a screening protocol in rural India areas and the examined subjects were entire families, consisting of parents and their children. This caused a gap between the two groups when age is reported in the horizontal axis. The fact that children were considered in this study can also explain the poorer correlation between the IMT measurements and the BMI, which has a different meaning when considering children. Numerical results, which confirmed the very good agreement between AELR and the Reader's measurements, can be found in Table II.

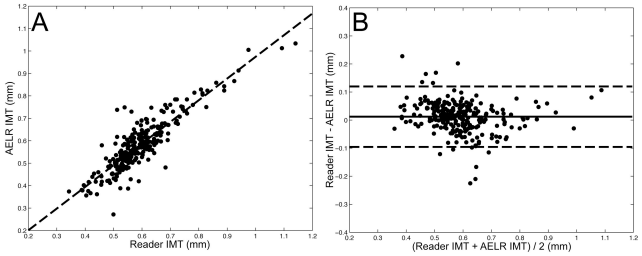

Fig. 2. Agreement between AELR and Reader IMT measurements. A) Correlation plot: the dashed line represents the linear regression. B) Bland-Altmann plot: the horizontal continuous line represents the IMT measurement bias and the dashed lines the average value ± 1.96 st. dev.

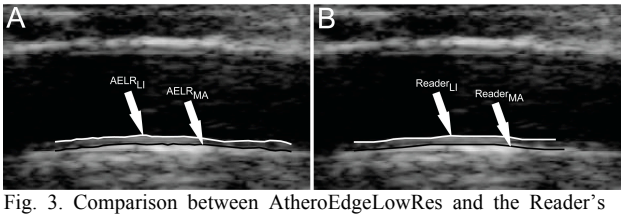

Fig. 3. Comparison between AtheroEdgeLowRes and the Reader's LI/MA tracings.

IV. DISCUSSION

In this paper we used an optimized automated image processing technique based on snakes to measure the IMT of a set of low-resolution and low-quality ultrasound carotid images. The results in terms of IMT measurement accuracy were benchmarked w.r.t. the values obtained by an expert sonographer.

From a technical point of view, our segmentation strategy brought innovation because it was the first of its kind to introduce the penalty factor correction. This correction optimized the position of the computer traced LI/MA boundaries by comparing the average positioning error to that of human tracings. This correction was needed in this specific study because: (1) The image dataset was of overall very low quality, in particular the images had a low pixel density, leading to a pixel physical dimension of 0.0787 mm/pixel. (2) The OEM acquisition scanner was low-end, thus the overall contrast and the representation of the LI/MA interfaces was often poor, causing inaccuracies in the computer automated tracings that needed correction; (3) The dataset was relative to mainly healthy subjects (since it was

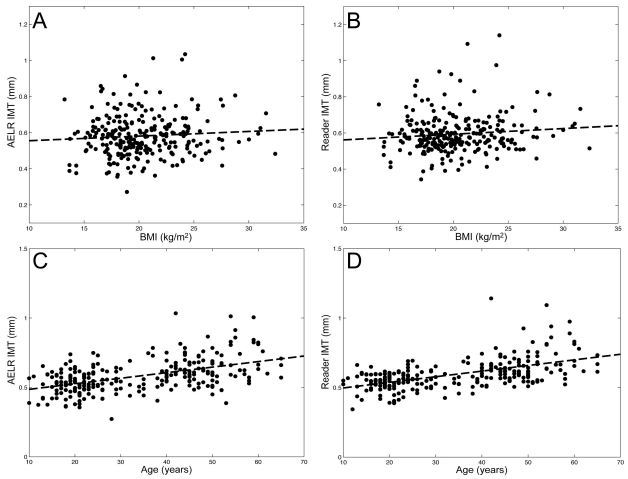

Fig. 4. Correlation plots between the IMT measurements and the subjects' BMI (*panels A and B*), and between the IMT measurements and the subjects' age (*panels C and D*). Panels A and C report the AtheroEdgeLowRes values, Panels B and D the Reader values.

a screening study), with average IMT equal to about 0.604 ± 0.129 mm (as measured by the Reader). This further increased the need for a very accurate and optimized measurement system.

Without the PF correction the average IMT measurement of AELR was 0.431 ± 0.075 mm, against the average IMT value by the Reader that was 0.604 ± 0.129 mm. Hence, the IMT measurement bias was 0.173 ± 0.127 mm, meaning about the 29% error on the nominal value of the IMT. Figure 1 highlights the increased IMT measurement accuracy obtained with the PF correction.

The IMT measurement performance of the PF corrected version of AELR reached, on this low-quality (?) and low-resolution dataset, similar performance of other automated techniques (see [8]) and of semi-automated ones [14]. The best performing technique we found in literature was proposed by Faita *et al*. [14]. The IMT measurement bias was 0.001 ± 0.035 mm, approximately 10 times lower than the error we had. However, the images were acquired by a medium/high-end scanner, MyLab25 (EsaoteSpA, Genova, Italy).

Table II reports the AELR and the Reader's IMT values split into groups. We observed agreement between the Reader's values and AELR values and we did not observe statistically significant difference. AELR IMT values were higher for subjects having hypertension, diabetes, heart disease, stroke, and asthma with respect to their respective controls. This is a very important result, showing the capability of AELR in maintaining the subjects' risk factors, thus providing very accurate and reliable results.

V. Conclusions

We developed a penalty factor (PF) correction dual-snake segmentation system that we applied to a set of 512 ultrasound limited-contrast and low-resolution carotid images coming from a screening study conducted in India. The need for a PF correction was justified by the low quality and resolution of the ultrasound images, acquired using a low-end OEM scanner. The automated computer IMT measurements were accurate and correlated with those manually obtained by an expert sonographer. We showed that the computer IMT measurements also preserved the subjects' risk factors. We believe that automated computer tracings have good enough accuracy and reproducibility to be used in large epidemiological and screening studies, even in emerging countries, where often the quality of the ultrasound scanner is lower.

References

[1] J. Labreuche, P. J. Touboul, and P. Amarenco, "Plasma triglyceride levels and risk of stroke and carotid atherosclerosis: a systematic review of the epidemiological studies," *Atherosclerosis,* vol. 203, no. 2, pp. 331-45, Apr, 2009.

[2] F. Molinari, K. M. Meiburger, G. Zeng *et al.*, "Automated carotid IMT measurement and its validation in low contrast ultrasound database of 885 patient indian population epidemiological study: results of AtheroEdge software," *International Angiology,* vol. 31, pp. 42-53, 2012.

[3] H. Schargrodsky, R. Hernandez-Hernandez, B. M. Champagne *et al.*, "CARMELA: assessment of cardiovascular risk in seven Latin American cities," *Am J Med,* vol. 121, no. 1, pp. 58-65, Jan, 2008.

[4] T. Naqvi, "Ultrasound vascular screening for cardiovascular risk assessment. Why, when and how?," *Minerva Cardioangiol,* vol. 54, pp. 53-67, 2006.

[5] J. F. Polak, L. C. Funk, and D. H. O'Leary, "Inter-reader differences in common carotid artery intima-media thickness: implications for cardiovascular risk assessment and vascular age determination," *J Ultrasound Med,* vol. 30, no. 7, pp. 915-20, Jul, 2011.

[6] C. Xu, and J. L. Prince, "Snakes, shapes, and gradient vector flow," *IEEE Trans Image Process,* vol. 7, pp. 359-369, 1998.

[7] F. Molinari, K. M. Meiburger, L. Saba *et al.*, "Fully automated dual-snake formulation for carotid intima-media thickness measurement. A new approach," *J Ultrasound Med,* vol. 31, no. 1123-1136, 2012.

[8] F. Molinari, G. Zeng, and J. S. Suri, "A state of the art review on intima-media thickness (IMT) measurement and wall segmentation techniques for carotid ultrasound," *Computer Methods and Programs in Biomedicine,* vol. 100, pp. 201-221, 2010.

[9] T. J. Dick, I. A. Lesser, J. A. Leipsic *et al.*, "The effect of obesity on the association between liver fat and carotid atherosclerosis in a multi-ethnic cohort," *Atherosclerosis*, 2012.

[10] F. Molinari, K. M. Meiburger, L. Saba *et al.*, "Ultrasound IMT measurement on a multi-ethnic and multi-institutional database: Our review and experience using four fully automated and one semi-automated methods," *Comput Methods Programs Biomed*, (in press).

[11] L. Saba, F. Molinari, K. M. Meiburger *et al.*, "What is the correct distance measurement metric when measuring carotid ultrasound intima media thickness automatically?," *Int Angiol,* vol. 31, pp. 483-489, 2012.

[12] F. Molinari, C. Pattichis, G. Zeng *et al.*, "Completely Automated Multi-resolution Edge Snapper (CAMES) : A New Technique for an Accurate Carotid Ultrasound IMT Measurement: Clinical Validation and Benchmarking on a Multi-Institutional Database.," *IEEE Trans Image Process*, pp. Sep 23. [Epub ahead of print], 2011.

[13] P. J. Touboul, M. G. Hennerici, S. Meairs *et al.*, "Mannheim carotid intima-media thickness consensus (2004-2006). An update on behalf of the Advisory Board of the 3rd and 4th Watching the Risk Symposium, 13th and 15th European Stroke Conferences, Mannheim, Germany, 2004, and Brussels, Belgium, 2006," *Cerebrovasc Dis,* vol. 23, no. 1, pp. 75-80, 2007.

[14] F. Faita, V. Gemignani, E. Bianchini *et al.*, "Real-time measurement system for evaluation of the carotid intima-media thickness with a robust edge operator," *J Ultrasound Med,* vol. 27, no. 9, pp. 1353-61, Sep, 2008.